Indian Journal of Chemistry
Vol. 53A, July 2014, pp. 816-819

Notes

Synthesis of single crystal zeolite L rods with high aspect ratio using rice husk ash as silica source

Rituparna Das, Sourav Ghosh & Milan Kanti Naskar*
Sol-Gel Division, CSIR-Central Glass & Ceramic Research Institute, Kolkata 700 032, India
Email: milan@cgcri.res.in

Received 21 April 2014; revised and accepted 20 June 2014

Single crystal zeolite L rods with high aspect ratio have been prepared using rice husk ash as silica source in the presence of other aqueous-based precursors via a single-step hydrothermal process at 170 ^{o}C for 72 h. Crystallization behavior of the particles is studied by X-ray diffraction, and the characteristic vibration bands of zeolite L are confirmed by FTIR spectroscopy. BET surface area and total pore volume of the particles are found to be 142 m^2 g^{-1} and 0.19 cm^3 g^{-1}, respectively. Rod-shaped morphology of zeolite L with an aspect ratio of 10-50 is observed by FESEM and TEM. Selected area electron diffraction pattern of TEM confirms the single crystal nature of the particles.

Keywords: Aluminosilicates, Zeolite L, Rice husk ash, Hydrothermal synthesis, Crystallization, Microstructure

Zeolite L (LTL) is a crystalline aluminosilicate with a typical chemical composition of $K_9Al_9Si_{27}O_{72}.nH_2O$ (n= 0-36).[1] It possesses one-dimensional channels with a 12-membered ring pore channel openings of 0.71×0.71 nm^2, which consists of cancrinite (CAN) cages and double six-membered rings (D6R) hexagonal prism connected alternatively along *c*-axis, with the [001] length forming a column.[1,2] Due to its unique structural features, ion exchange capabilities and high thermal stability, it is widely used in catalysis, host-guest chemistry[2,3] and selective gas adsorption.[4] The size and morphology affect its performance in different applications. Rod-like morphology of zeolite L is important in the applications of microcapillary devices for light harvesting antenna and luminescent labeling.[5] Zeolite L has been synthesized with tunable size and morphology using colloidal silica as the silica source.[6-10] There are a few reports on the synthesis of zeolite L from rice husk ash.

Rice husk is an abundantly available agriculture waste materials containing maximum amount of siliceous ash. Burning of rice husk in air produces rice husk ash (RHA) containing 85-98% silica. The burnt rice husk causes environment pollution and health hazard. Therefore, useful applications of rice husk are desirable to mitigate environment pollution and health hazard. Yusof *et al.*[11] synthesized faujasite and NaA-type zeolites using rice husk ash. Zeolite beta has also been obtained from rice husk ash.[12] Wong *et al.*[13] prepared nanocrystalline zeolite L particles using rice husk ash as silica source via a multi-step process.

Keeping in view the above, in the present work, we have synthesized zeolite L via ***in situ*** extraction of silica from RHA in the presence of other low cost aqua-based precursors like aluminum foil, potassium hydroxide and water without using a templating agent. In this process, we could overcome the separate extraction process of silica from rice husk ash. Herein, we have obtained single crystal zeolite L rods with a high aspect ratio. The present method is important in terms of low cost as well as environmentally-friendly process.

Experimental

The starting materials were rice husk ash (locally collected with the composition (wt%): SiO_2 (95.54), Al_2O_3 (0.78), K_2O (0.72), P_2O_5 (1.45), MgO (0.60), CaO (0.29), Fe_2O_3 (0.23), Na_2O (0.10), MnO (0.05), TiO_2 (0.02) and SO_3 (0.22), potassium hydroxide (GR, Merck, India, purity>98%), aluminium metal foil (SD Fine-Chem Ltd., India) and deionized water.

In a typical experiment, the Al foil (0.257 g) was dissolved in 60 mL of potassium hydroxide (0.9 *M*) solution under stirring to obtain a clear solution followed by addition of 3 g RHA. This particulate suspension was stirred for 20 h at room temperature (30 ^{o}C). The molar composition of the mixture was maintained as $10SiO_2:Al_2O_3:5.7K_2O:700H_2O$. After stirring for 20 h, the mixed suspension was hydrothermally treated at 170 ^{o}C for 24 h, 48 h and 72 h. The resulting solid masses were then washed with deionized water repeatedly until *p*H of the washed liquid became almost neutral. Finally, the samples were dried at 80 ^{o}C for 6 h.

The thermal behavior of the samples was studied by differential thermal analysis (DTA) and thermo-gravimetry (TG) (Netzsch STA 449C, Germany) from 30 to 800 ^{o}C in air atmosphere at the heating rate of 10 ^{o}C min^{-1}. The crystal phases of the particles were identified using powder diffraction technique by a

Philips X'Pert Pro XRD (model PW 3050/60) with Ni-filtered Cu-K radiation (= 0.15418 nm), operating at 40 kV and 30 mA. The characteristic vibration bands of the particles were confirmed by FTIR (Nicolet 5PC, Nicolet Analytical Instruments, Madison, WI) by KBr pellet method at a resolution of 4 cm^{-1} and scan rate of 100 spectra sec^{-1}. Nitrogen adsorption-desorption measurements were conducted at 77 K with a Quantachrome (ASIQ MP) instrument. The samples were outgassed in vacuum at 250 ^oC for 4 h, prior to the measurement. The total surface area was determined by the BET method. Micropore (pore size < 20 Å) volume was calculated by the t-plot method. The total pore volume was estimated from the amount of nitrogen adsorbed at the relative pressure (*p/po*) of ~0.99. The Barrett-Joyner-Halenda (BJH) method was employed to calculate the pore size distribution in the mesopore range while differential pore volume distributions in the micropore range were evaluated by the DFT method. The morphology of the synthesized particles was examined by FESEM (model Zeiss, Supra^{TM} 35VP, Oberkochen, Germany) operating with an accelerating voltage of 10 kV, and TEM using a Tecnai G2 30ST (FEI) instrument operating at 300 kV.

Results and discussion

The DTA and TG analyses of the sample prepared hydrothermally at 170 ^oC for 72 h are shown in Fig. 1. The DTA curve of the sample shows a broad endothermic peak at around 200 ^oC accompanied with a sharp weight loss of about 4%, up to 200 ^oC as evidenced by the TG curve. The TG analysis also shows a total weight loss of about 6.5% up to 800 ^oC. The endothermic peak and the weight loss are attributed to the removal of adsorbed water in the sample. Figure 2 shows the XRD patterns of the samples synthesized at 170 ^oC for 24, 48 and 72 h. Up to 48 h of reaction time, the characteristic peak of -quartz at 2 26.7^o present in RHA was seen. However, for 72 h of synthesis time at 170 ^oC, crystallization of Linde type zeolite L (LTL) (JCPDS File No. 43-560) was observed. To investigate the vibrational characteristics of the bonds found in the samples, FTIR spectra were recorded (Supplementary data, Fig. S1). The characteristic absorption bands of zeolite L were absent for the samples prepared after 24 and 48 h reaction time. However, for 72 h reaction time, the absorption peaks appeared at 440, 580, 649, 716, 783, 1080 and 1116 cm^{-1}, confirming the presence of zeolite L. These results support the XRD data. The bands at 1080 and 1116 cm^{-1} indicate asymmetric stretching modes of T-O-T (T = Si, Al), and those at 716 and 783 cm^{-1}correspond to the symmetric stretching vibration of internal tetrahedral as well as external linkages. The double six ring (D6R) in the framework structure of zeolite L was confirmed by the absorption bands at 580 and 649 cm^{-1}. The band at 440 cm^{-1} was ascribed to T-O bending vibration as well as the characteristic pore opening of external linkages of zeolite L.[3]

The N_2 adsorption and desorption isotherms of zeolite L synthesized at 170 ^oC for 72 h, show that the initial steep micropore uptake takes place at about *p/po*<0.02 (Fig. 3). The uptake of nitrogen increases steeply above the relative pressure of ~ 0.8, showing an IUPAC type IV isotherm in which the hysteresis loops are due to the formation of textural mesoporosity originated from the intergrowth of the crystals.[14] The mesopores generated during the

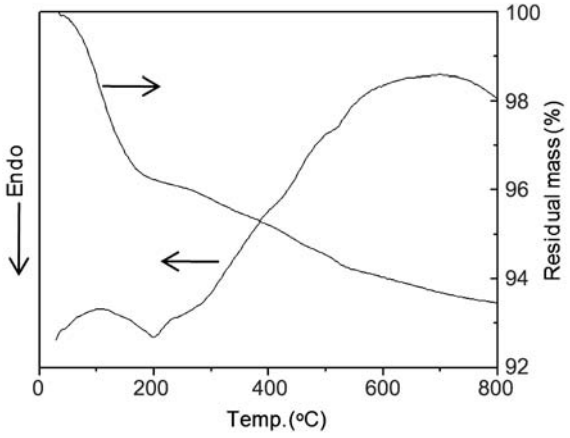

Fig. 1—DTA and TG curves of zeolite L synthesized at 170 ^oC for 72 h.

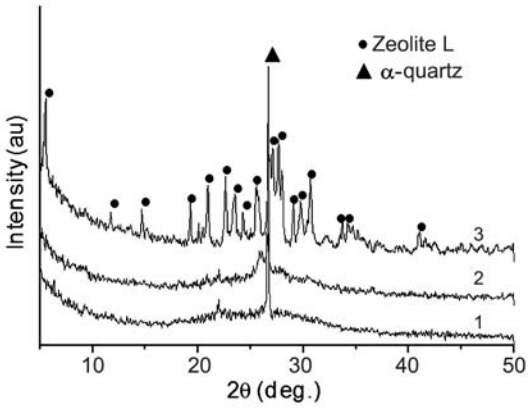

Fig. 2—XRD patterns of the particles. [1, -quartz; 2, -quartz; 3, zeolite L].

formation of zeolite crystals have a slit-like shaped. The zeolite L sample showed BET surface area and total pore volume of 142 m^2 g^{-1} and 0.19 cm^3 g^{-1}, respectively. The BET surface area comprised the external surface area of 69 m^2 g^{-1} and micropore surface area of 73 m^2 g^{-1}. It is clear that the external surface area originated from interparticle pores which were developed by particle-particle aggregation, while the micropore surface area was due to the intrazeolitic (structural) pores of zeolite. The pore size distributions (PSDs) of zeolite L are depicted in Fig. S2 (Supplementary data). It was observed that in the micropore range as evaluated by DFT method (Fig. S2(a)), the maximum differential pore volume was recorded at about 7.3 Å, very close pore diameter of zeolite L (7.1 Å). The BJH pore size distribution curve (Fig. S2(b)) derived from the adsorption data of the isotherm shows a prominent peak at around 50.5 Å, indicating the generation of mesopores in the synthesized zeolite L particles.

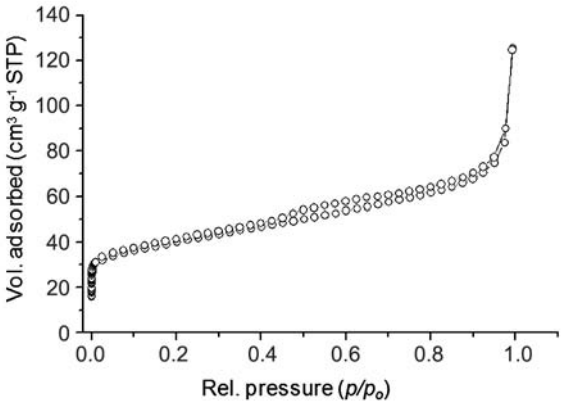

Fig. 3—Nitrogen adsorption and desorption isotherms of zeolite L.

Figure 4(a) shows the FESEM image of the particles obtained hydrothermally at 170 °C for 72 h. It reveals the rod-shaped morphology of zeolite L of length of 2-5 m with the diameter ranging from 100–200 nm. The aspect ratio of the particles is in

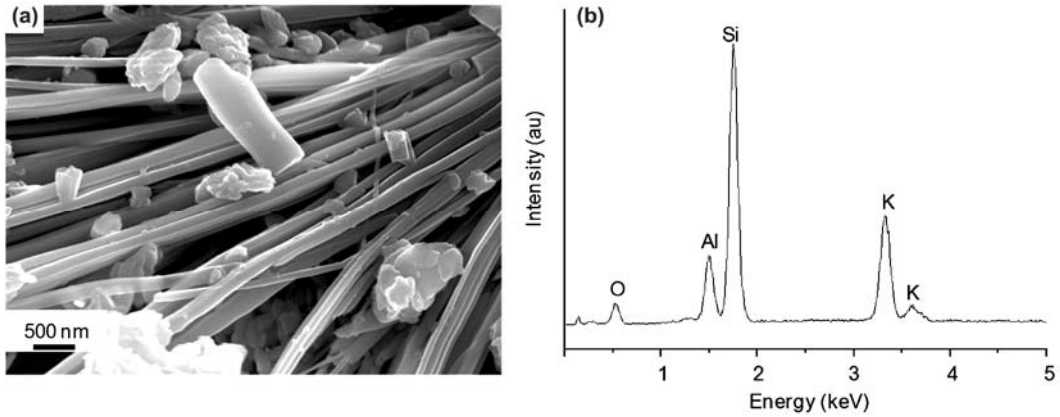

Fig. 4—(a) FESEM image and (b) EDX of zeolite L synthesized at 170 °C for 72 h.

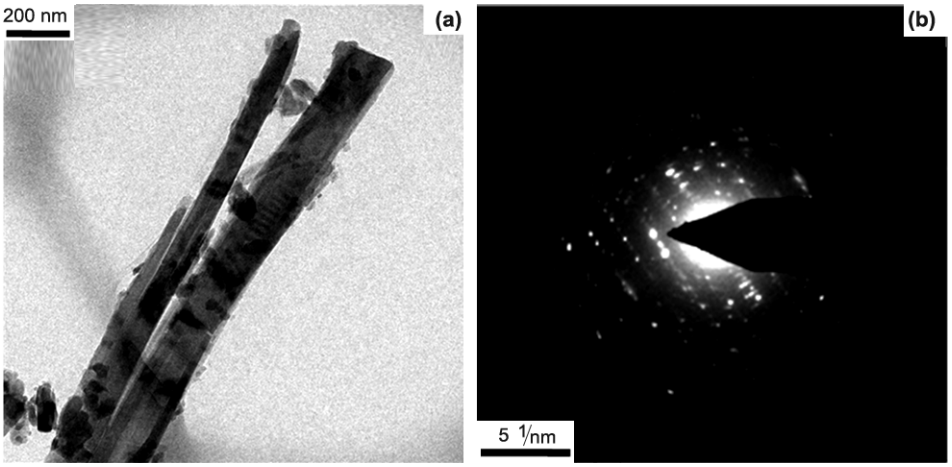

Fig. 5—(a) TEM image and (b) SAED pattern of zeolite L synthesized at 170 °C for 72 h.

the range of 10-50, and much higher than the reported data. The elemental analysis of zeolite L studied by EDX analysis (Fig. 4(b)) indicates the Si/Al ratio of 4.6, which is close to the stoichiometric composition taken as the precursor. Interestingly, for the synthesis time of 24 and 48 h at 170 ^{o}C, the samples revealed particulate nature (Supplementary data, Fig. S3). The TEM image (Fig. 5(a)) also confirms the rod shaped morphology of zeolite L. The cross-sectional view (indicated with an arrow mark) of zeolite L rod is shown in Fig. S4 (Supplementary data). The selected area electron diffraction (SAED) pattern (Fig. 5(b)) of zeolite L shows single crystal indicating parallel lines joining the diffraction spots. The elongated diffraction spots in the zeolite L rod indicate the presence of multiple nanodomains with a small misorientation. The presence of multiple nanodomains causes a random alignment among nanocrystallites in the zeolite L rods.[15,16]

In this study, we report the synthesis of single crystal zeolite L rods of high aspect ratio (10-50) by direct extraction of the agrowaste material (RHA) in the presence of aqua-based precursors without using a templating agent. The locally available agrowaste material (RHA), which is environmentally hazardous, can be exploited to yield a value added product like zeolite L in an economic and environmentally friendly process.

Supplementary data

Supplementary Data associated with this article, i.e., Figs S1-S4, are available in the electronic form at http://www.niscair.res.in/jinfo/ijca/IJCA_53A(07)816-819_SupplData.pdf.

Acknowledgement

RD and SG are thankful to University Grants Commission (UGC), New Delhi, India, and Council of Scientific and Industrial Research (CSIR), New Delhi, India, respectively for their fellowships. The financial support from CSIR under the project no. CERMESA-ESC-0104 is also thankfully acknowledged.

References

1 Breck D W, *Zeolite Molecular Sieves: Structure, Chemistry and Use*, (Wiley, New York) 1974.
2 Matsunaga C, Uchikoshi T, Suzuki T S, Sakka Y & Matsuda M, *Mater Lett*, 93 (2013) 408.
3 Ko Y S & Ahn W S, *Bull Korean Chem Soc*, 20 (1999) 1.
4 Dangi G P, Munusamy K, Somani R S & Bajaj H C, *Indian J Chem*, 51A (2012) 1238.
5 Maas H, Khatyr A & Calzaferri G, *Micropor Mesopor Mater*, 65 (2003) 233.
6 Lee Y-J, Lee J S & Yoon K B, *Micropor Mesopor Mater*, 80 (2005) 237.
7 Ruiz A Z, Bruhwiler D, Ban T & Calzaferri G, *Monat Chem*, 136 (2005) 77.
8 Gomez A G, Silveira G D, Doan H & Cheng C-H, *Chem Comm*, 47 (2011) 5876.
9 Insuwan W & Rangsriwatananon K, *Eng J*, 16 (2012) 1.
10 Lupulescu A I, Kumar M & Rimer J D, *J Am Chem Soc*, 135 (2013) 6608.
11 Yusof A M, Nizam N A & Rashid N A A, *J Porous Mater*, 17 (2010) 39.
12 Prasetyoko D, Ramli Z, Endud S, Hamdan H & Sulikowski B, *Waste Manag*, 26 (2006) 1173.
13 Wong J-T, Ng E-P & Adam F, *J Am Ceram Soc*, 95 (2012) 805.
14 Majano G, Darwiche A, Mintova S & Valtchev V, *Ind Eng Chem Res*, 48 (2009) 7084.
15 Zhang Z, Sun H, Shao X, Li D, Yu H & Han M, *Adv Mater*, 17 (2005) 42.
16 Ghosh S, Roy M & Naskar M K, *Mater Lett*, DOI: 10.1016/j.matlet.2014.06.045.